Electronic Supplementary Information

Supramolecular - Directed Synthesis of RNA-Mediated CdS/ZnS Nanotubes†

Anil Kumar*[a,b] and Vinit Kumar[a]

[a]Department of Chemistry and [b]Centre of Nanotechnology
Indian Institute of Technology Roorkee, Roorkee - 247667, **India**
E-mail: anilkfcy@iitr.ernet.in; Tel.: +91-1332-285799; Fax: +91-1332-273560

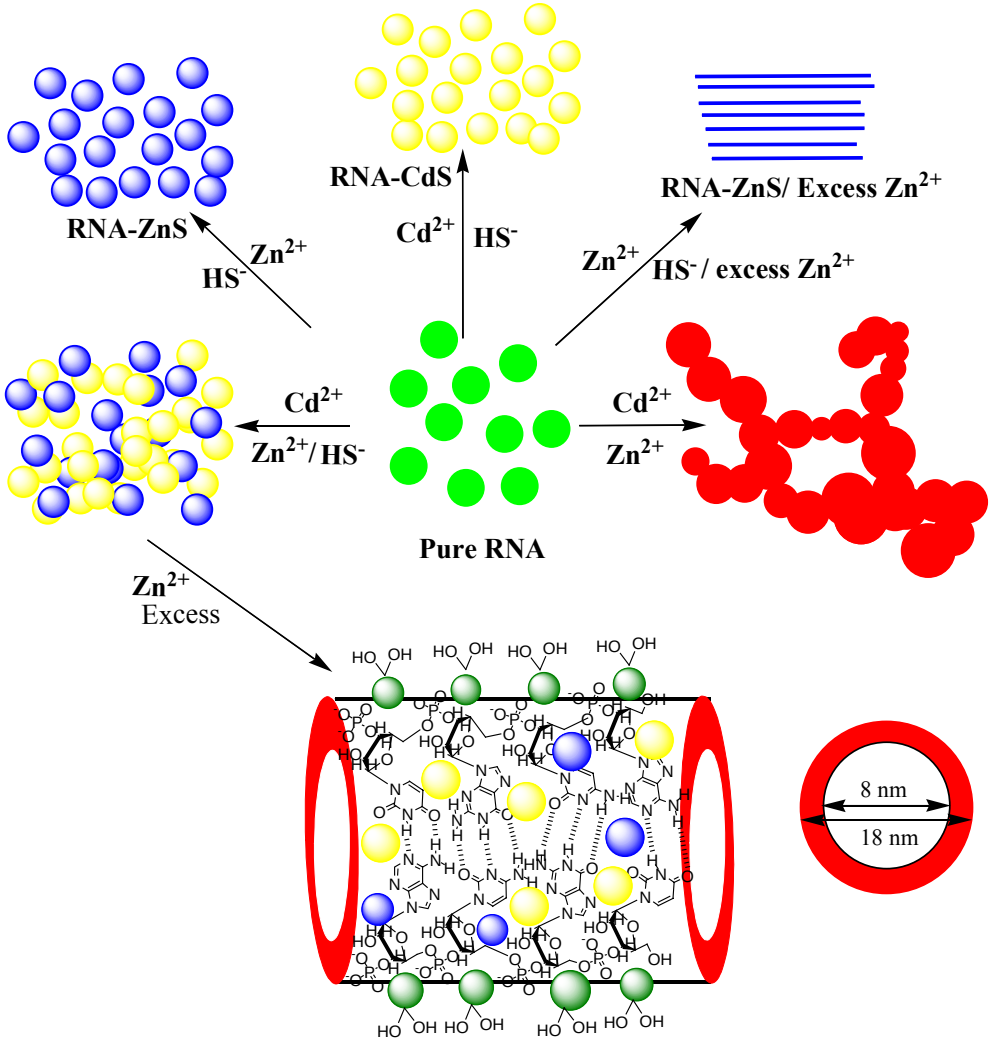

Nanotubes

Scheme S1

Experimental Section

Materials. Zinc acetate (Fluka); cadmium perchlorate (Aldrich) and RNA (Sigma); NaOH (Qualigens); acridine orange, perchloric acid, FeS (Merck) were all of analytical grade. All these chemicals were used without any further purification. Nitrogen with purity >99.9% (Sigma) was used for deoxygenating the solution during synthesis.

The used RNA (Type VI) was derived from Torula Yeast containing phosphorous contents of ~ 8.5%. Further, this is a heterogeneous mixture of RNA molecules with varied molecular weights.

Equipment. Absorption and emission spectra were recorded on Shimadzu UV-2100S spectrophotometer and Shimadzu RF-5301-PC spectrofluorophotometer, respectively at room temperature. AFM images were recorded on a NTEGRA (NTMDT). Electron microscopy and SAED analysis were performed on a FEI-TECNAI Digital TEM having variable magnification 1100,000X working at 200 keV. The surface morphology of nanotubes was determined by a FEI-QUANTA 200F field emission scanning electron microscope coupled with energy dispersive X- ray. Fluorescence lifetime and anisotropy decay curves were recorded on a Horiba Jobin Yvon-IBH single photon counter in time domain mode. NanoLEDs (340 nm) and LDs (400 nm) were used as excitation sources. The emitted photons were detected by Hamamatsu (R 3809 U) photomultiplier and thermoelectrically cooled TBX-04-D detector. IR spectra were obtained on a Thermo Nicolet Nexus FTIR spectrophotometer in mid IR range in KBR medium. X-Ray diffraction patterns were recorded on a Philips DW 1140/90 X-ray diffractometer using Cu Kα line (1.5418 Aº) of the X-Ray source.

Synthesis of RNA-mediated CdS/ZnS colloidal solution

RNA templated CdS/ZnS nanotubes were synthesized by injecting freshly prepared SH^- (2.5×10^{-4} mol dm^{-3}) to the deaerated aqueous solution of RNA (0.015g /100 ml) containing 20µl solution of each $Cd(ClO_4)_2$ and $Zn(CH_3COO)_2$ from their respective stock solutions (0.1 mol dm^{-3}) at pH 9.2. After the addition of SH^-, 70 µl of additional amount of $Zn(CH_3COO)_2$ (0.1 mol dm^{-3}) was further injected to this reaction mixture under constant purging of N_2 at room temperature. The final pH of solutions was adjusted to 9.2. **It thus results in the coprecipitation of CdS and ZnS simultaneously to produce CdS/ZnS co-colloids**. The onset of absorption, excitonic absorption and emission maximum were found to get blue shifted with increasing amount of RNA (Figure S1a). These particles were unstable at a pH ≤ 8.5 and the emission intensity is reduced to about 20% at a pH 9.8. On the other hand an addition of increasing amount of Zn^{2+} ($1x10^{-4}$ to $7x10^{-4}$ mol dm^{-3}) to the CdS/ZnS co-colloids resulted in a small but regular red shift in the onset of absorption and excitonic peak. It, however, causes a significant increase in the intensity of emission associated with a blue shift in the emission maximum from 520 nm (2.38 eV) to 509 nm (2.44 eV) (Figure S1b).

Characterization:

For TEM analysis sample(s) were prepared by applying a drop of the colloidal solution on to a carbon coated copper grid for 2 min. Excess solution was removed by a tissue paper.

Atomic force microscope operating under semi-contact mode was used to analyze surface topography of the synthesized nanomaterials keeping the resonance frequency at 280 kHz. All AFM images were recorded at room temperature. The AFM instrument was

calibrated with a standard specimen (Diffraction grating TDG01) with an average surface roughness ≥ 50nm. Surface morphology was also examined by FESEM coupled with EDX. Samples for AFM and FESEM analysis were prepared by applying a drop of colloidal solution on to a glass plate and then drying it under vacuum at room temperature. Acridine orange was used as a reference dye for the determination of quantum efficiency of the synthesized material. Fluorescence decay curves were analyzed using DAS6 software provided from IBH. Anisotropy was calculated directly from the decay curves employing the method given in the below reference.[1]

1. DAS6-3 manual user guide; HORIBA JOBIN YVON.

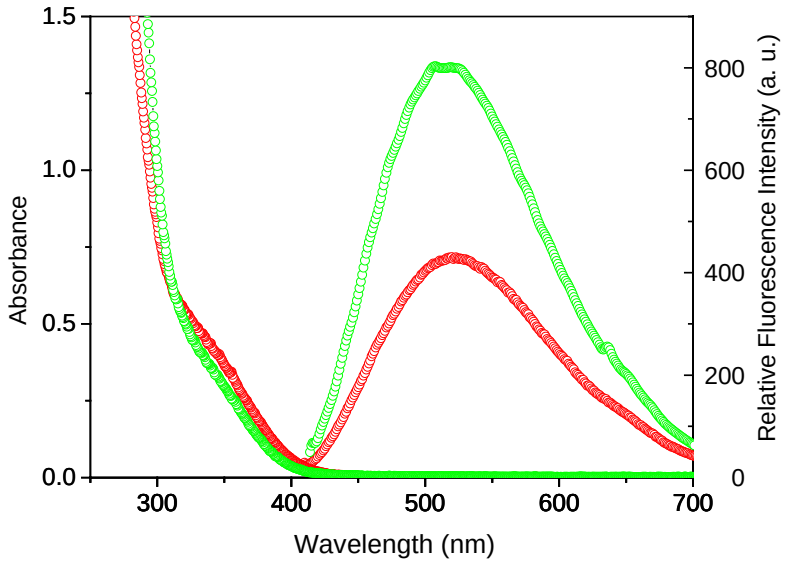

Figure S1a: Effect of the amount of RNA on the electronic and emission spectra of CdS/ZnS; 0.005g (red), 0.015g (green). [λ_{ex}= 400 nm]

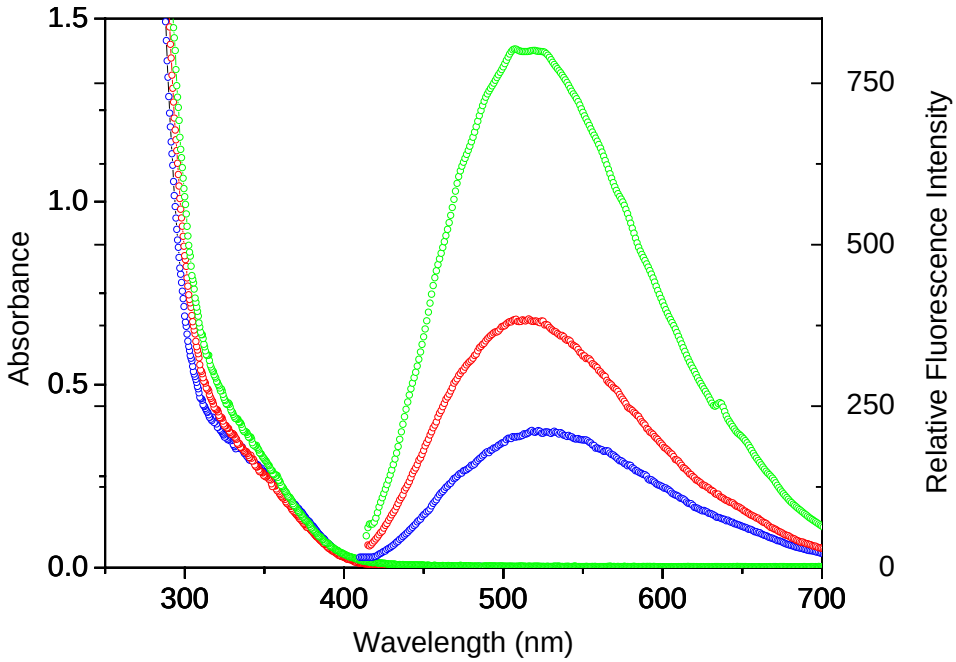

Figure S1b: Electronic and emission spectra of sample SP1 (Green), SP2 (Blue) and SP3 (red). [λ_{ex}= 400]

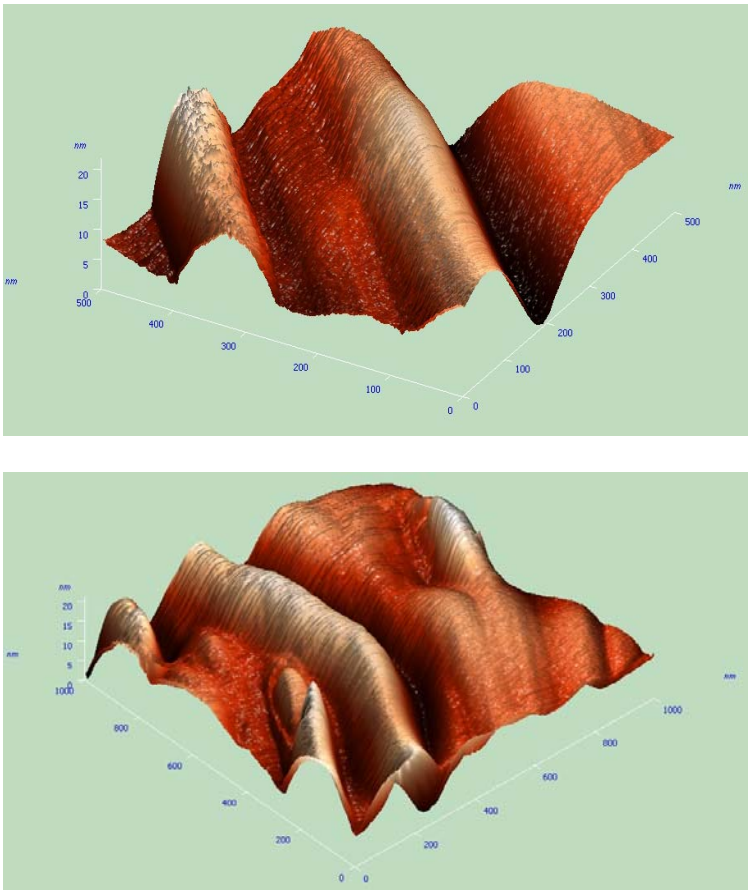

Figure S2: AFM images of nanotubes.

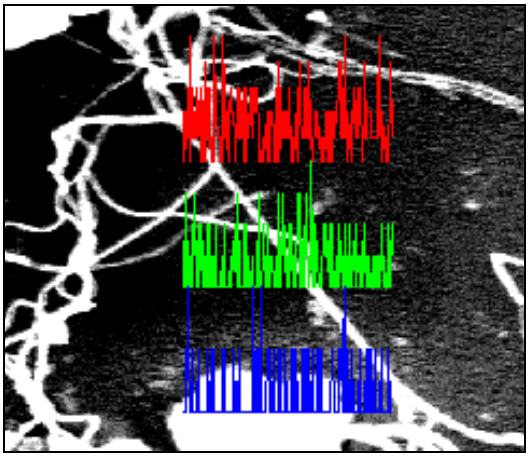

Figure S3: EDX of nanotube depicting homogenous distribution of S (green); Cd (red) and Zn (blue) along the tube.

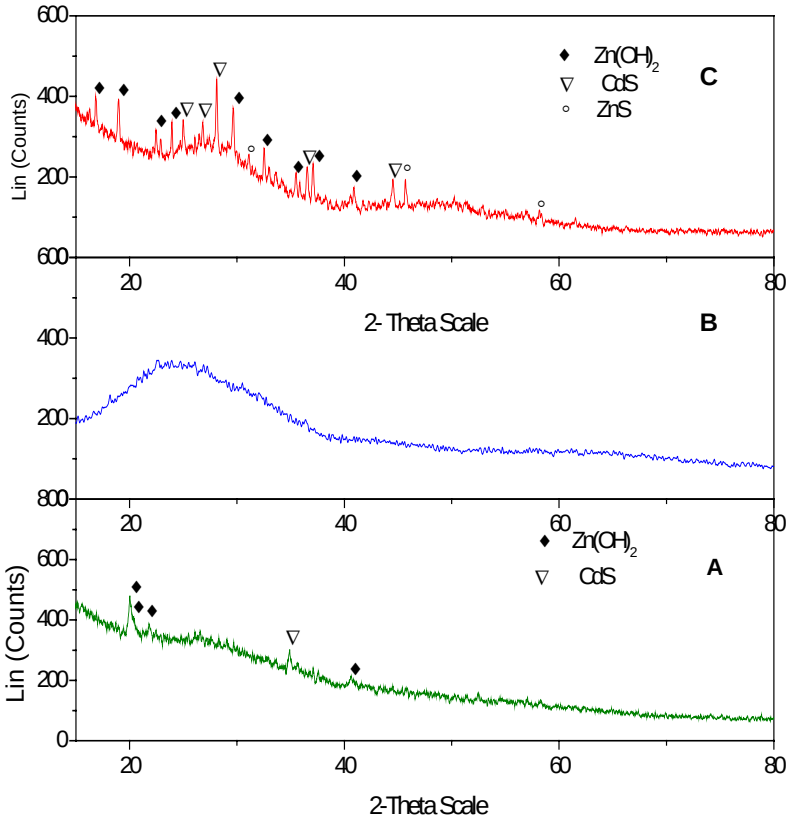

Figure S4: XRD patterns of R2 (A), as prepared colloidal solution of **SP1** (B) and powder sample of **SP1** (C).

XRD pattern of R2 (penal a) correlates to'd' spacing corresponding to $Zn(OH)_2$ [(301), (302), (116), (424), (028)] and $Cd(OH)_2$ [(011] in orthorhombic and hexagonal phases, respectively. XRD pattern of **SP1** correlates to 'd' spacing corresponding to CdS [(100), (002), (101), (102), (110)]; ZnS [(101), (102), (110), (201)]; $Zn(OH)_2$ [(112), (113), (116), (305), (008), (317), (028), (119), (231)] in hexagonal, wurtzite and orthorhombic phases, respectively. It may be mentioned that the hydroxide of both Cd^{2+} and Zn^{2+}could be seen only in XRD pattern of R2 (penal a). However, no reflection corresponding to $Cd(OH)_2$ is observed in XRD patterns of SP1 (penal b).

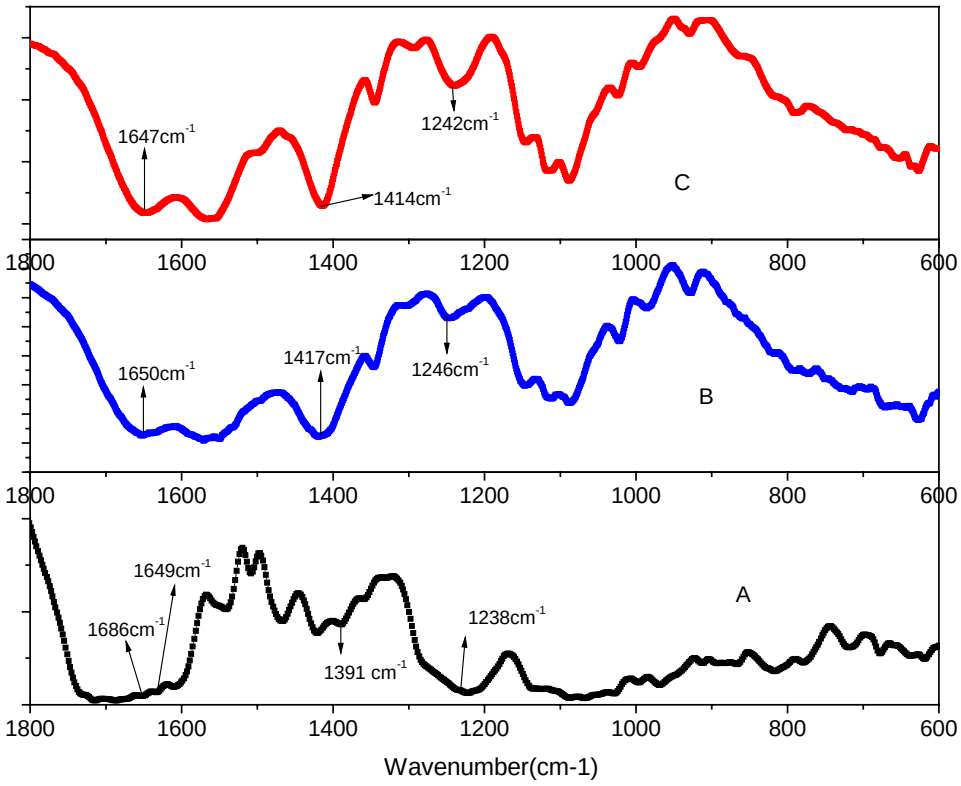

Figure S5: FTIR spectra of R1 (A); R2 (B); SP1 (C).

Table S1: IR spectral data of R1, R2 and SP1.

Group / Moiety	**RNA (R1) (cm^{-1})**	**Cd^{2+}+Zn^{2+}-RNA (R2) (cm^{-1})**	**(CdS+ZnS)-RNA SP1 (cm^{-1})**
U, G, A and C	1750-1600(br)	1650(w)	1647(s)
PO_2^{2-}	1238(sh)	1246(m)	1242(s)
2′-OH	1391 (w)	1417 (m)	1414(s)

s-strong; m- medium; w- weak; sh- shoulder; br- broad.

IR spectrum of pure RNA (R1) exhibits various vibrational bands at 1750-1600 cm^{-1}, 1391 cm^{-1} and 1238 cm^{-1} and, which corresponds to nucleobases (A, U, G and C), sugar-phosphate (PO_2^-) and sugar moiety (2′-OH) of RNA, respectively (Table S1, figure S4, ESI).[2] RNA in the presence of excess Cd^{2+}/Zn^{2+} (R2) results in a significant change in the absorption frequencies of various functional groups/moieties suggesting their interaction with Cd^{2+}/Zn^{2+}.

2. (a) Arakawa, H.; Neault, J. F.; Tajimir-Riahi, H. A. *Biophysical Journal,* 2001, **81**, 1580- 587; (b) M. Banyay, M. Sarkar and A. Gräslund, *Biophysical Chemistry*, 2003, **104**, 477-488.

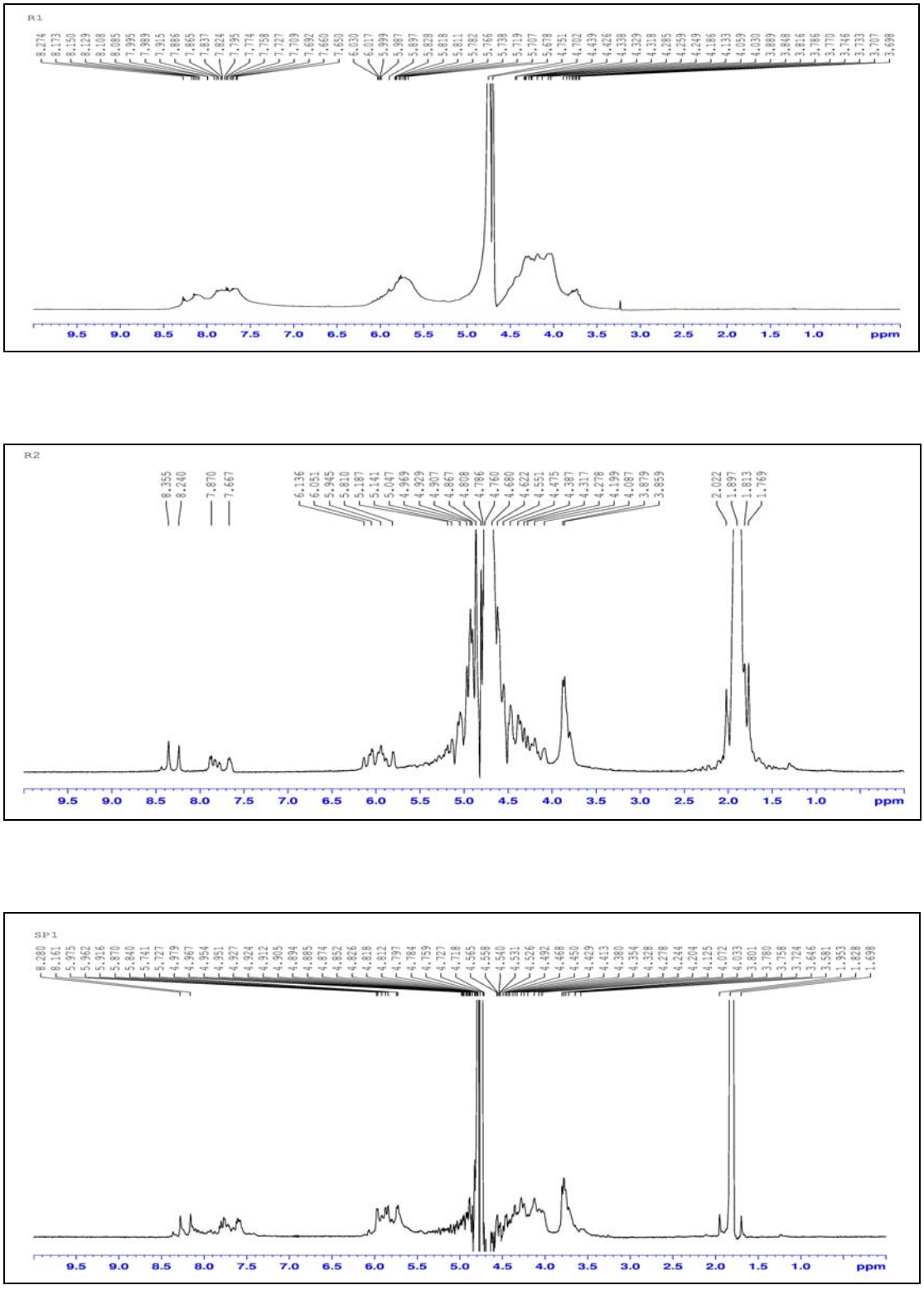

Figure S6: ^{1}H NMR of pure RNA (R1), RNA-Cd^{2+}/Zn^{2+} (R2) and RNA-CdS/ZnS (SP1).

The ^{1}H NMR of R1 exhibits all the characteristic peaks due to sugar protons (H_2', H_3', H_4', H_5', H_5''), purine and sugar base (H_1', H_5) and aromatic protons of purine and pyrimidine bases (H_2, H_8, H_6) resonating between 4 to 4.5, 5 to 6 and 7 to 8.3 ppm, respectively similar to that of reported earlier.[3] The addition of Cd^{2+} and Zn^{2+} ions to RNA causes all the peaks due to different moieties to be better resolved with a small decrease in δ (ppm). Besides, an additional peak appears due to 2′-OH of sugar at 1.9 ppm possibly due to reduced exchange of this proton upon complexation with Cd^{2+} and Zn^{2+}.

3. B. Fürting, C. Richter. C, J. Wöhnert and H. Schwaibe, *Chem. Bio. Chem.*, 2003, **4**, 936.

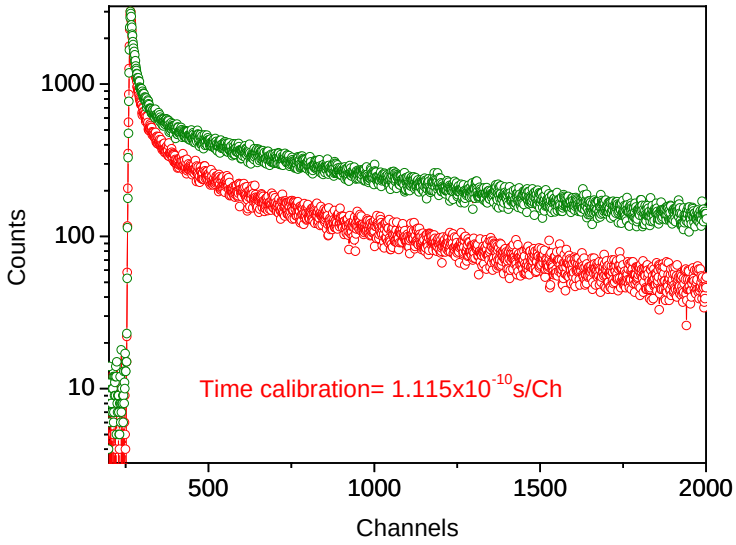

Figure S7a: Fluorescence decay curves of SP1 (olive) and SP2 (red). [λ_{ex}= 405 nm; λ_{em}= 509 nm].

Table S2:
Lifetimes of SP1 and SP2. [λ_{ex} = 405 nm; λ_{em} = 509 nm]

	Component 1		component 2		component 3		<τ >	χ^2
Sample	**τ_1 (ns)**	**Emission %**	**τ_2 (ns)**	**Emission %**	**τ_3 (ns)**	**Emission %**	**(ns)**	
SP1	6.2 (0.0391)	15.5	83.3 (0.0236)	9.4	0. 8 (0.1897)	75.1	70	1.1
SP2	5.8 (0.0389)	14.0	57.7 (0.0152)	5.6	0.7 (0.2223)	80.4	41	1.1

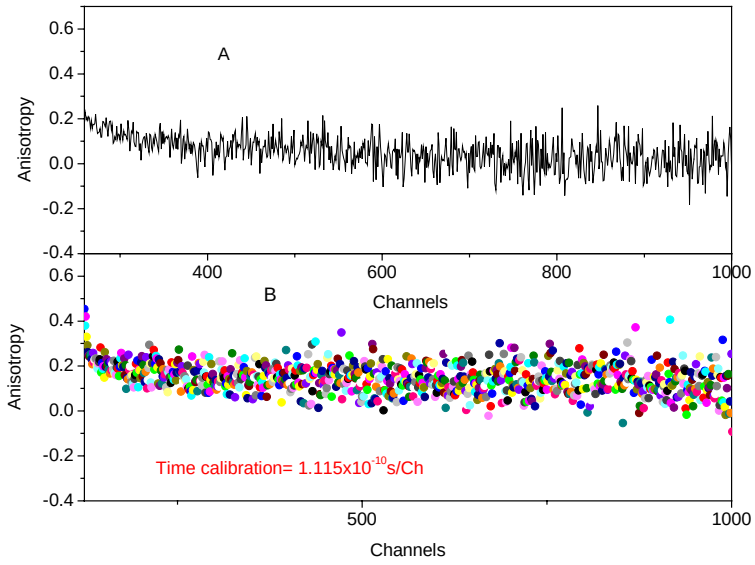

Figure S7b: Fluorescence anisotropy decay curves of sample SP2 (A) and SP1 (B). [λ_{ex}= 405 nm; λ_{em}= 509 nm]

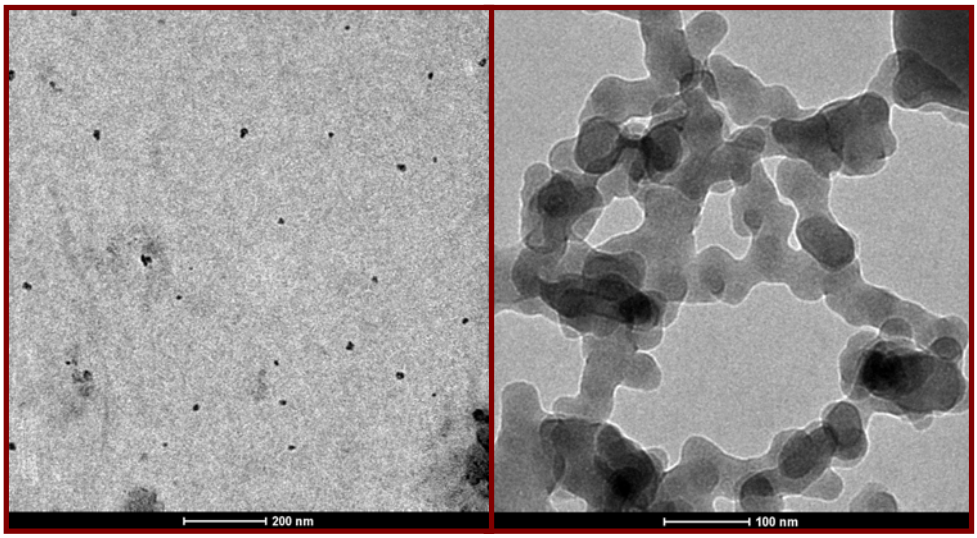

Sample R1 (A) Sample R2 (B)

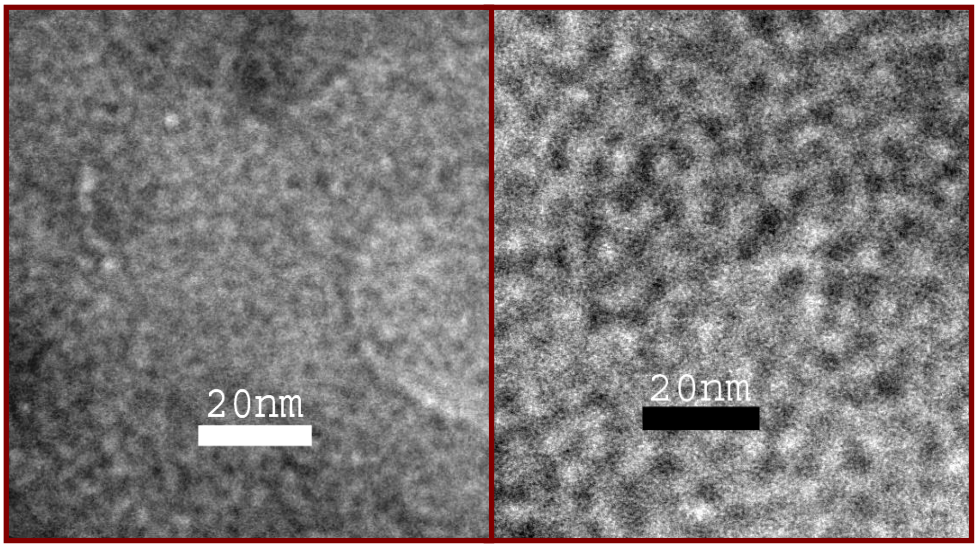

Sample SP2 (C) Sample SP3 (D)

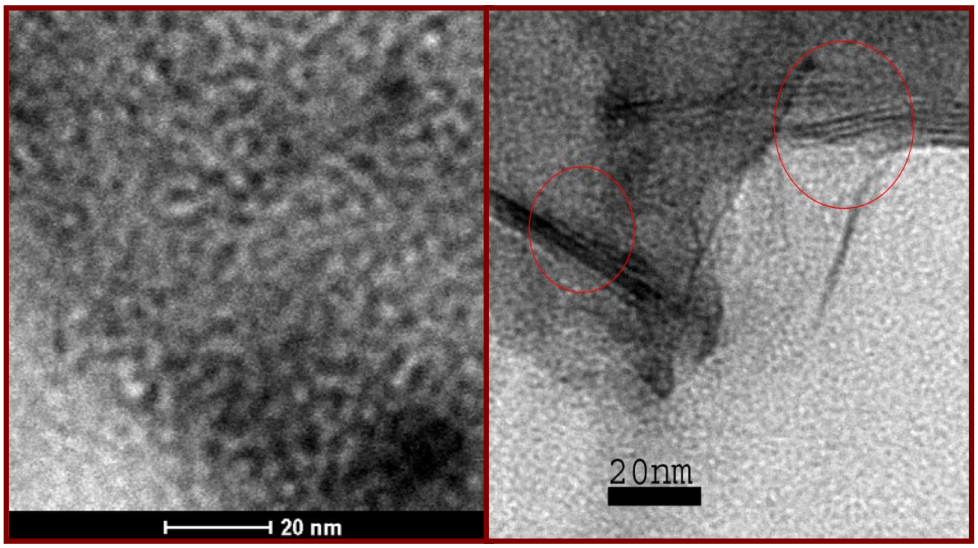

E F

Figure S8: TEM images of precursors and some other possible intermediates namely, pure RNA (A), RNA consisting Cd^{2+} and excess Zn^{2+} ions (B). These images show that under the used experimental conditions pure RNA contains particle size 7nm whereas in the presence of Cd^{2+} and excess Zn^{2+} ions it exhibit the formation of bigger cluster having a diameter of 42 nm. RNA-templated ZnS with (F) and without excess Zn^{2+} (E), RNA-CdS/ZnS (C) without excess Zn^{2+} and with smaller amount of excess Zn^{2+} (D) were prepared under the used experimental conditions. RNA-templated ZnS without excess Zn^{2+} consists of spherical particles of ZnS having an average diameter of 2.2 nm. In the presence of excess Zn^{2+} it formed **multiple layered nanowires** having an average diameter of 0.7 nm.